J Sol-Gel Sci Technol (2018) 85:269–279
DOI 10.1007/s10971-017-4546-1

ORIGINAL PAPER: EDUCATIONAL ASPECTS OF SOL-GEL AND HYBRID MATERIALS

Study of thermal and flame behavior of phosphorus-based silica for epoxy composites

Vibha Shree[1] · **A. K. Sen**[1]

Received: 11 September 2017 / Accepted: 10 November 2017 / Published online: 20 November 2017

Abstract Phosphorous-containing silica was prepared by acid hydrolysis of sodium silicate via a cost-effective sol–gel method. Phosphorus was incorporated during synthesis of silica by adding three different phosphorus compounds namely di-sodium hydrogen orthophosphate, orthophosphoric acid, and hypophosphorous acid. The silica powder was analyzed by Fourier transform infrared spectroscopy (FTIR), thermogravimetric analysis (TGA), scanning electron microscopy (SEM), and dynamic light scattering (DLS). FTIR spectrum shows the presence of phosphorous in the samples. SEM picture of phosphorous containing silica is globular whereas pure silica is fluffier. The EDX results indicate the phosphorous incorporation up to 5 wt% atomic weight. TGA analysis shows approximately 15 wt% loss up to 150 °C for oven dried samples and the residue at 700 °C is higher for phosphorous containing samples. DLS results show the particle size for all the samples near 1000 nm. Limiting oxygen index (LOI) and smoke density of the epoxy composite samples was evaluated. The LOI value of the phosphorous containing silica composite material has been slightly improved. But the burning behavior of the samples indicates the sufficient formation of protective char layer and the char analysis of the composite samples shows more bubble structure. This type of foam structure of the char protects the surface from fire propagation.

✉ A. K. Sen
akhilsen@bitmesra.ac.in
akhilsen@yahoo.co.in

[1] Department of Chemical Engineering, Birla Institute of Technology, Mesra, Ranchi 835215, India

Graphical abstract

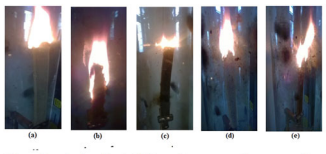

Burning behavior of Pure Epoxy and composites (a) Ep (b)ESI (c)ESHPA (d)ESOPA (e)EDSHP

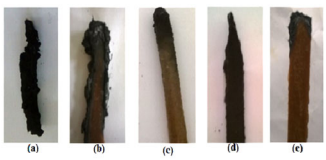

Photos of burnt sample after LOI test for pure Epoxy and composites (a) Ep (b) ESI (c) ESHPA (d) ESOPA (e) EDSHP

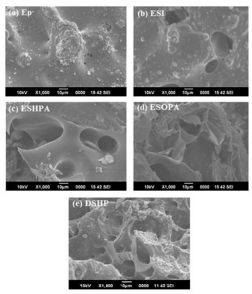

SEM of char formed of burnt sample after LOI test for pure Epoxy and

Ep=Epoxy network
ESI=Epoxy + Silica composites
ESHPA=Epoxy+Silica(H3PO4)
ESOPA= Epoxy + Silica (H3PO2)
EDSHP= Epoxy + Silica (NaH2PO4)

Keywords Phosphorus · Silica · Sol–gel · Flame retardant · SEM

1 Introduction

Polymer systems have considerable attention due to their unique properties, such as low cost, lightweight, and easy fabrication. Among these, epoxy resin (Ep) is an influential thermoset having properties like marvelous thermal stability with excellent chemical resistance, which ensures their large applications in various areas of adhesives, coating, electronic/electrical insulation, etc. However, the main disadvantage of the resin are their high flammability, which confines their applications requiring high flame resistance; especially in electrical and electronic

application. The addition of flame retardants is an effectual method to depress the polymer flammability. There are two feasible approaches to achieve flame retardancy one is additive type and another is reactive approach [1–5].

In the past decades, brominated compounds have been widely used as a flame retardant. These have excellent flame retardant capacity due to higher trapping efficiency and lower decomposing temperature. They are active through the gas phase by releasing halogen radicals, which react with free oxygen and hydroxyl radicals responsible for the chain reaction of burning organic gases. However, they evolve very toxic and corrosive gases (e.g., polybrominated dibenzo-p-dioxins, furans) in the case of fire, incineration or recycling [6–10].

The growths of environmental concern over halogenated flame retardants have raised interest in the use of phosphorous based flame retardants (PFR) since 1970. Their versatility, ease of preparation and eco-profile, has encouraged the development of phosphorus-based fire retardants for epoxy resins [11]. The PFRs are applied in a variety of products, such as textile, floor polish, and lacquers. Phosphorous compounds are available as phosphate, phosphonate, phosphinate, and phosphine oxide and also as oxyacids in different oxidation state (+1, +3, +4, and +5) [12, 13]. PFRs work both in solid phase and in the gaseous phase. The flammable gases like $H^{\cdot}$ and OH^{-} are engulfed in the gas phase because of the formation of active radicals like PO, PO_2, and HPO hence reducing the energy of the flame. Moreover, in the solid phase, they form a protective and heat resistant carbonaceous residue or char. Thermogravimetric (TG) analysis of these compounds shows the charring behavior of phosphorous-based compounds. As reported by Schartel [13] phosphinate oxide compound shows more phosphorous containing gas release whereas in the case of phosphates mainly charring are found [14].

In recent years, there has been considerable interest in phosphorous containing silica because of the synergic effect of the two. The joint impact amongst phosphorus–silicon containing elements could be advantageous to resist the thermal degradation of the resin consequently, reduce flammability to a greater extent [15, 16]. Alongi et al. studied thermal and flame retardant behavior of coated phosphorous-doped silica over cotton fabrics [17]. They observed a significant reduction of burning rate and time of the coated cotton fabrics. However, in most of the cases, costly organosilicates and organophosphates are used for silica preparations.

Therefore, this study aims to incorporate phosphorus compound into silica particles through a cost-effective sol–gel method from cheap materials (sodium silicate). During this synthesis of silica, a polymeric stabilizer (polyvinyl alcohol) and small quantity phenol are used to get narrow distribution of particle size. Three different phosphorous containing agents are chosen namely, hypophosphorous acid (+1 oxidation state), orthophosphoric acid (+5 oxidation state), and disodium hydrogen phosphate (+5 oxidation state). It has been hypothesized that incorporation of such modified silica could increase the thermal stability and fire retardant behavior of the resin. The characterization is done by using FTIR, SEM, DLS, XRD, porosity, and TGA. Composites are prepared by using epoxy resin and the silica filler. The fire retardant behavior and thermal stability of composites are characterized through TGA, LOI, and smoke density.

2 Experimental

2.1 Materials

Sodium silicate (Loba Chemie), polyvinyl alcohol (PVA, Mol. Wt. 85,000–1,24,000, S.D. Fine Ltd.), Hydrochloric acid were used for acid hydrolysis of sodium silicate. The phosphorous containing agents used were disodium hydrogen orthophosphate dihydrate ($Na_2HPO_4{\cdot}2H_2O$, S. D. Fine Ltd.), orthophosphoric acid (H_3PO_4, RFCL Ltd.), and hypophosphorous acid (H_3PO_2 Loba Chemie). Phenol and distilled water were used in this work. Bisphenol A-based epoxy resin (LAPOX B-11), and amine-based hardener (K6, *N*, *N*′-Bis (2-aminoethyl) ethane-1, 2-diamine) was used for composite preparation.

2.2 Preparation of phosphorous-containing silica filler

Phosphorous-containing silica was prepared by sol–gel technique [18, 19]. The reaction was carried out in 1 l round bottom flask equipped with stirrer, thermometer, and dropping funnel. Two-hundred milliliter of distilled water and polyvinyl alcohol (2 g) was added into it and stirred until it dissolves. Sodium silicate (30 g) was dissolved in 100 ml of water in a separate beaker and the solution was added in to the above PVA solution. The mixture was then heated to 60 °C and stirred continuously. Phenol (9.9 g) was added into the reaction mixture with continuous stirring. Next, 2N HCl was added dropwise in stirring condition. When the solution appeared cloudy the phosphorous containing compounds (disodium hydrogen phosphate, hypophosphorous acid, and ortho phosphoric acid) were added in three subsequent batches followed by HCl addition up to pH 1. The amount of these phosphorous-containing compounds were calculated so that the Si:P = 1. The heating and stirring were continued for 2 h. Thus three samples of phosphorous-containing silica were prepared. One blank silica samples was prepared by the above method for comparison. The mixture was then left overnight to settle down the precipitate. It was then washed, filtered, and dried

Table 1 Nomenclature of pure silica and phosphorous-containing silica

Sample description	Abbreviations	Resin	Composite
Pure silica	SI	Epoxy	ESI
Phosphorous-doped silica using hypo-phosphorous acid	SHPA	Epoxy	ESHPA
Phosphorous-doped silica using ortho-phosphoric acid	SOPA	Epoxy	ESOPA
Phosphorous-doped silica using di-sodium hydrogen orthophosphate	DSHP	Epoxy	EDSHP

in air oven until constant weight at temperature 100 °C. The white powder thus obtained was crushed in a ball mill for 10–12 h. The possible reaction scheme is as follows and the sample nomenclatures are shown in Table 1.

$$Na_2SiO_3 + H_2O \longrightarrow Si(OH)_4 + 2NaCl$$

$$Si(OH)_4 + H_3PO_4 \longrightarrow \text{-O-Si-O-P-O-} + H_2O$$

2.3 Preparation of composites

Epoxy resin was mixed with the filler and then degassed in a vacuum oven for 30 min. The hardener was added in 10:1 (by wt.) ratio and stirred for 15 min. It was then poured into the channels of dimension 120 × 15 × 3 mm in PTFE mold and left for 24 h for curing at room temperature. The strips were then kept in hot air oven for 2 h at 120 °C for final curing [20]. The sample nomenclatures are shown in Table 1.

2.4 Instrumental analysis and measurements

FTIR spectra of the silica filler were recorded in SHIMADZU make IR Prestige 21 model spectrophotometer. TGA analysis of the filler and composites were performed using a SHIMADZU make DTG60 model thermogravimetric analyzer. Samples were heated in a platinum pan from room temperature to 800 °C at a heating rate of 10 °C/min. The particle morphology of the silica filler was determined by scanning electron microscopy (SEM) using JSM 5800, JEOL. The EDS analysis was carried out to determine the amount of phosphorous in silica sample. The particle size of the powder silica samples was carried out in Malvern particle size analyzer nano ZS model. The porosity of the silica powder was determined by Mercury Porosity Meter, Thermo electronics, Italy, PASAL 440 model. XRD patterns of the filler were obtained in a Rigaku, Japan, Smart Lab 9 kW diffractometer working with Cu-Kα radiation in continuous mode between 2Θ, 0–80° with speed 10°/min. LOI was determined according to ASTM D 2863 by using CSI-178 Oxygen Index Tester. The specimen's dimensions are 70–150 mm length, 6.5 mm wide, and 3 mm thickness. Smoke density was determined according to ASTM D 2843 by using Smoke Density Test Apparatus manufactured by S. S. Instruments New Delhi with sample dimensions as 25 × 25 × 6 mm.

3 Results and discussion

3.1 Silica filler

3.1.1 FTIR analysis of silica

Figure 1 shows FTIR spectra of the synthesized phosphorous containing silica. The broad band between 3343 and 3200 cm^{-1} indicates the presence of hydrogen-bonded OH group. The peak near 1650cm–1600cm^{-1} is for O–H bending. The peak at 1138–1090 cm^{-1} and 470 cm^{-1} is for Si–O–Si asymmetric stretching and bending. The peak near 960–950 cm^{-1} is due to the stretching vibration of silanol groups [21, 22]. The peak near 1095 and 790 cm^{-1} is due to (P=O) and terminal P–O– or Si–O, respectively. Peak in the range of 470 cm^{-1} is due to Si–O–Si bending.

3.1.2 Thermogravimetric analysis of silica

Figure 2 shows the TGA thermograms of pure and phosphorous-containing silica. There is a continuous weight loss from 30 to 700 °C. The weight loss from room temperature to 100 °C is low (nearly 3–6wt %) due to physically adsorbed water on the surface of silica particles. The weight loss from 100 to 700 °C is nearly 20–24wt% (Table 2). This is attributed to the condensation of silanol groups or elimination of degradation products at the higher temperature. The residue is much more in the case of phosphorous containing silica in comparison to pure one throughout the temperature range. At 700 °C, the residue for pure silica is 76 wt% whereas for phosphorous containing silica it is about 78–80 wt%. The slightly higher residue is due to the presence of phosphorous which needs more oxygen (1:2.5 in P_2O_5) rather than silicon atom (1:2 in SiO_2).

3.1.3 Scanning electron microscopy of silica

The surface morphology of the silica samples is shown in Fig. 3. The micrograph of pure silica shows fluffy structure

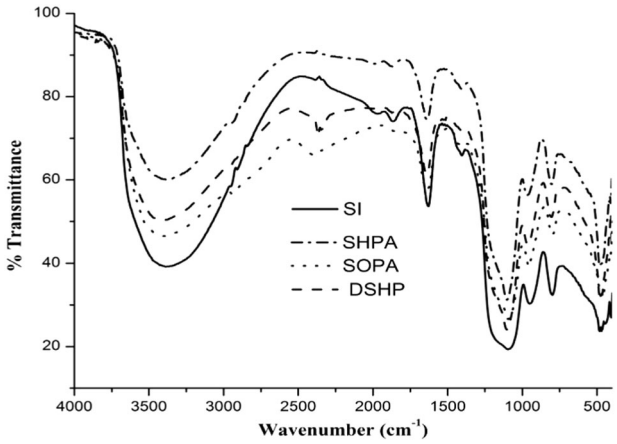

Fig. 1 FTIR spectrum of phosphorous-based silica

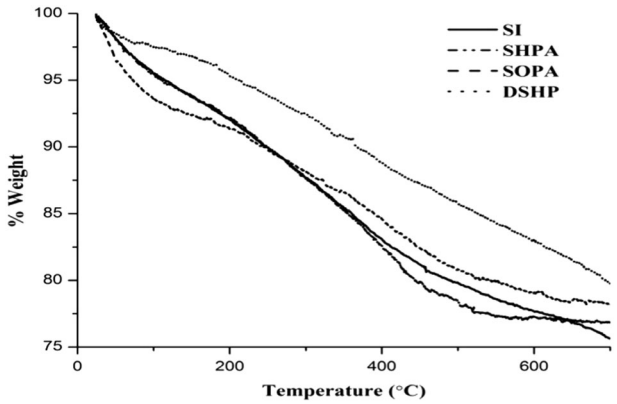

Fig. 2 TG curve for silica and phosphorous containing silica

Table 2 TGA of pure silica and phosphorous containing silica

Samples	%Weight loss		Residual char at 700 °C
	At 100 °C	At 700 °C	
SI	4.5	24	76
SHPA	6.4	22	78
SOPA	4.5	23	77
DSHP	2.5	20	80

whereas phosphorous containing samples show globular morphology. This is due to the condensation of the hydroxyl group of phosphorous with silicon which leads to the formation of agglomerated structure. The agglomerates are smaller and more closely packed [23, 24].

The physicochemical properties of the silica powder were measured and shown in Table 3. The specific surface area of the particles in $m^2\,g^{-1}$ was calculated using following equation:

$$S_p = \frac{6}{\gamma_p D_p},$$

where D_p is the average particle diameter and γ_p is specific density assumed to be $2.0 \times 10^6\ g^{-3}$ for amorphous silica particles. Again the specific densities of the silica particles were measured from their weight to volume ratio using the formula

$$\gamma_p = \frac{M}{V},$$

where M is the mass of the sample measured with micro-balance (10^{-5} g accuracy), and V is the volume measured by filling the silica particles in a column of known quantity.

3.1.4 EDX of phosphorous-based silica

The atomic percentage of oxygen, silicon, and phosphorous are shown in Table 4. This show phosphorous is present in all phosphorous-containing silica samples. This indicates that phosphorous has incorporated into the silica matrix. The atomic percentage of oxygen is much more in the case of phosphorous-containing silica in comparison to pure silica which is evident from TGA results also. This is due to presence of phosphorous which is present in oxide form in the solid. The presences of oxygen in Table 4 indicate that the silica is also present in the form of oxide [23, 25]. Figure 4 shows Si and phosphorous mapping of silica filler. It shows the homogenous distribution of phosphorous into the silica matrix.

3.1.5 Particle size by light scattering

The synthesized silica powders were dried in hot air oven near 100 °C and were ground in the ball mill for size reduction. The ground samples were dispersed in deionized water. It was then analyzed using cuvette cells, and the results were averaged over three consecutive runs. Figure 5 is the particle size result for pure silica and phosphorous-containing silica. The average particle size of silica is 733 nm, and that of phosphorous-containing silica is in the range of 1000 nm [26, 27].

3.1.6 Porosity of silica

Porosity is essential for many vital functions including thermal insulation and thermal shock resistance, but at the same time, the mechanical strength decreases with increase in the number of voids present [24]. The porosity of the silica samples was determined by filling the dilatometer with mercury along with the sample and pressurizing it by the instrument. It was found that the porosity of silica is about 35% whereas phosphorous containing silica is less than half. This is due to the condensation of hydroxyl group of phosphorous and silicon leading to more compacted structure (Table 5).

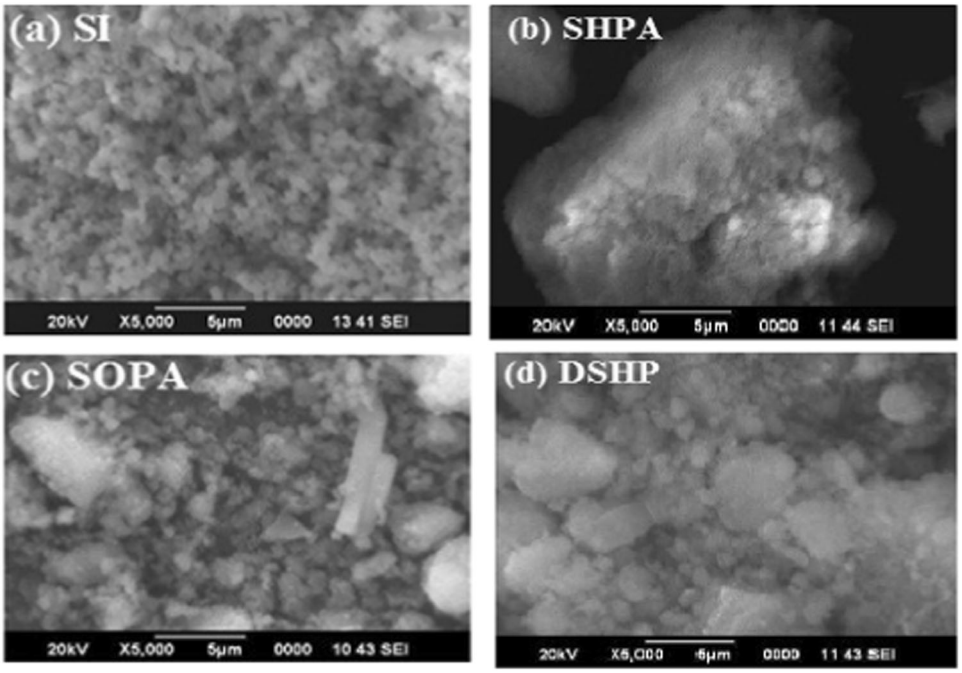

Fig. 3 SEM images of Phosphorous based silica

Table 3 Physicochemical characteristics of the silica

Samples	Bulk density (mg m^{-3})	Specific surface area (m^2 g^{-1})
SI	0.35	4.09
SHPA	0.31	4.16
SOPA	0.44	4.18
DSHP	0.40	4.8

Table 4 Result of EDX of phosphorous containing silica

SI		SHPA	SOPA	DSHP
Element	Atomic (%)	Atomic (%)	Atomic (%)	Atomic (%)
O K	52.86	59.08	61.38	53.18
Si K	39.18	35.26	34.37	44.64
P K		5.66	4.25	2.18

3.1.7 XRD of silica

Figure 6 shows the X-ray diffraction spectrum of the phosphorous containing silica powder. The broad hump between 2Θ, 10–20° is attributed to amorphous silica. The diffraction peaks obtained at 2Θ, 31, 45, and 56 are due to the formation of SiP_2O_7 phases as reported in the literature which is absent in pure silica sample [28]. SHPA has the lowest peak intensity compared to other phosphorous-containing samples. This is due to the lower hydroxyl content of hypophosphorous acid which acts as chain terminating agent. Whereas others have more hydroxyl group which reacts with neighboring hydroxyl group of silica leading to three-dimensional structure.

3.2 Epoxy-silica composites

3.2.1 Thermogravimetric analysis

The effect of phosphorous on thermal stability of epoxy resin and its composites were investigated by TGA in an air atmosphere. Figure 7a shows the TGA results of samples with the rate of heating is 10 °C/min. The pattern of the curves of neat Ep and composites shows three-stage thermal degradation. All the samples show the initial weight loss of about 5 wt% up to 250 °C. This is due to adsorbed water molecules and volatiles. The second stage weight loss starts from 250 °C and is continued up to 450 °C. At this stage maximum weight loss takes place. At 450 °C, Ep shows 90% degradation whereas epoxy-silica composites show 70% degradation. Between 450 and 650 °C, phosphorous-containing epoxy-silica composites show a delay in degradation behavior compared to epoxy-silica composites. At 650 °C the residue is 10–14 wt% higher for phosphorous-containing epoxy-silica composites than epoxy silica composites (Table 6). The retarded-degradation phenomenon is due to the phosphorous groups forming an insulating protective layer on the top and hence higher thermal stability and higher char yield [29–32].

The DTG graphs of composites are shown in Fig. 7b. The epoxy silica composites show early degradation peak

than the phosphorous-containing epoxy silica composites. This is due to acidic nature of silica which accelerates the degradation of the epoxy matrix. All the phosphorous-containing epoxy composites show a delay in degradation as is evident from the peaks positions.

3.2.2 Limiting oxygen index

Limiting oxygen index (LOI) is the minimum amount of oxygen required for a candle like burning of the samples. It is a small-scale standard test for characterizing the flammability tendency of materials [33, 34]. It is expressed regarding volume percentage of oxygen required to sustain the flame in a mixture of nitrogen and oxygen. The LOI value for epoxy resin (Ep) was 23 whereas for all other samples it was found to be 24. The lower increment in LOI values is due to lower phosphorous content.

Figure 8 shows the flame behavior of test samples after 60 s of ignition. Phosphorous containing epoxy silica composites are showing low flame characteristics than others. Also, flame propagation is faster for Ep and epoxy silica composites. Figure 9 is the burnt samples after extinguishing the flame for 120 s. This shows fire has propagated quickly in the two samples, whereas the major portion of the fire retardant samples are not affected by the fire. This is due to the char formation of fire retardant epoxy

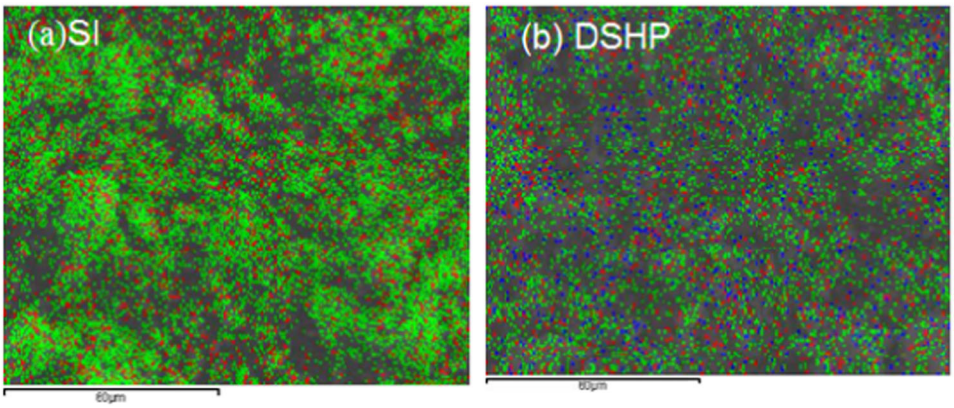

Fig. 4 Si and P mapping of silica fillers (silicon green color, oxygen red color and phosphorous blue color) (color figure online)

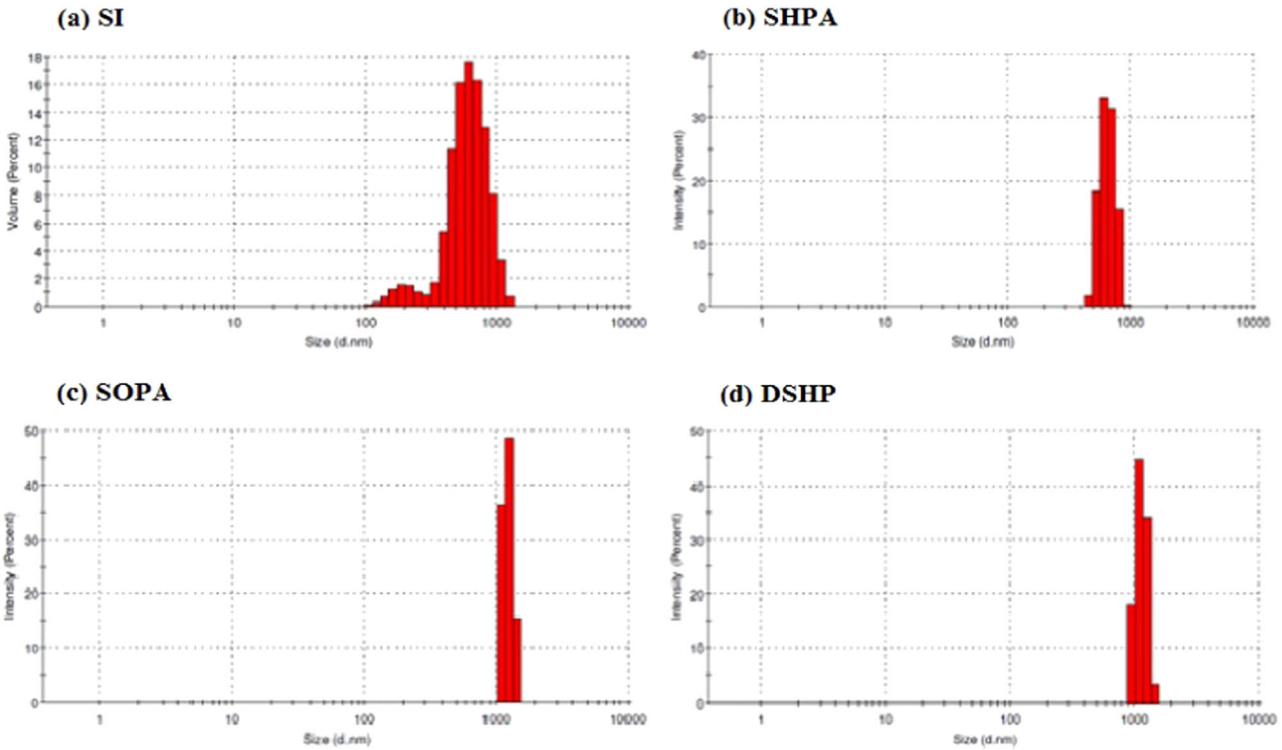

Fig. 5 Particle size of phosphorous-based silica

composite on the propagating surface. Char layer reduces the oxygen diffusion into the flame propagated surface due to which fire propagation was slow. However the charred layer of the samples could not act as a perfect barrier to shield the unburned polymer matrix against heat as well as hindering the diffusion of combustive gases.

Table 5 Porosity values of phosphorous-containing silica

Samples	Porosity
SI	34.4
SHPA	18.6
SOPA	14.2
DSHP	11.5

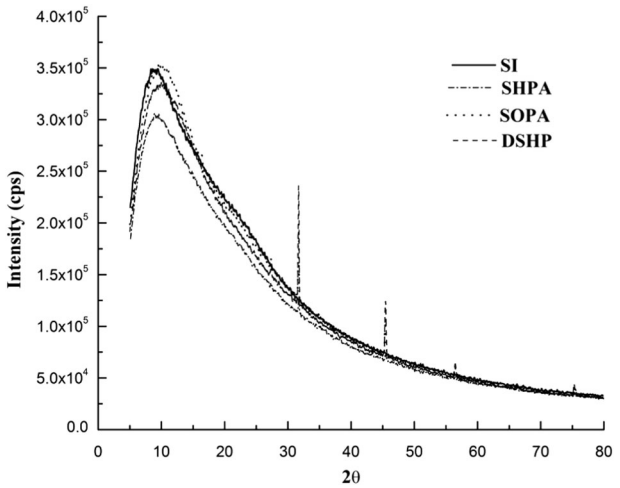

Fig. 6 XRD pattern of phosphorous-containing silica

3.2.3 SEM of burnt samples

Figure 10 is the SEM picture of the char formed after 120 s burning of epoxy samples from the LOI tests. Unfilled epoxy resin (Ep) is not showing any bubble while others have bubbles. Also, the sizes of the bubbles are much bigger for phosphorous containing silica samples. This is due to the formation of volatile gases during degradation of composites [35–37]. TGA analysis of silica filler (Fig. 2) shows continuous weight loss up to 700 °C. These volatiles are released during fire propagation makes the surface porous and voluminous.

Figure 11 is the element mapping of the top surface of burnt sample of epoxy-silica composites. It shows the presence of silica and phosphorous in the samples. This indicates that the phosphorous has incorporated in to silica matrix and the bubbles are generated from the loss of volatiles in the flame temperature [38, 39].

3.2.4 Smoke density

Smoke density is used to measure the response of materials, products or assemblies to heat and flame under controlled

Table 6 TG data of pure epoxy and composites

Samples	%wt. loss at 250 °C	%wt. loss at 450 °C	%wt. loss at 600 °C	DTG	Char residue (%) at 650 °C
Ep	4	85	97	384,634	0
ESI	4	78	100	376,530	0
ESHPA	2	65	79	404,601	9
ESOPA	4	68	80	409,618	10
EDSHP	5	69	86	391,592	14

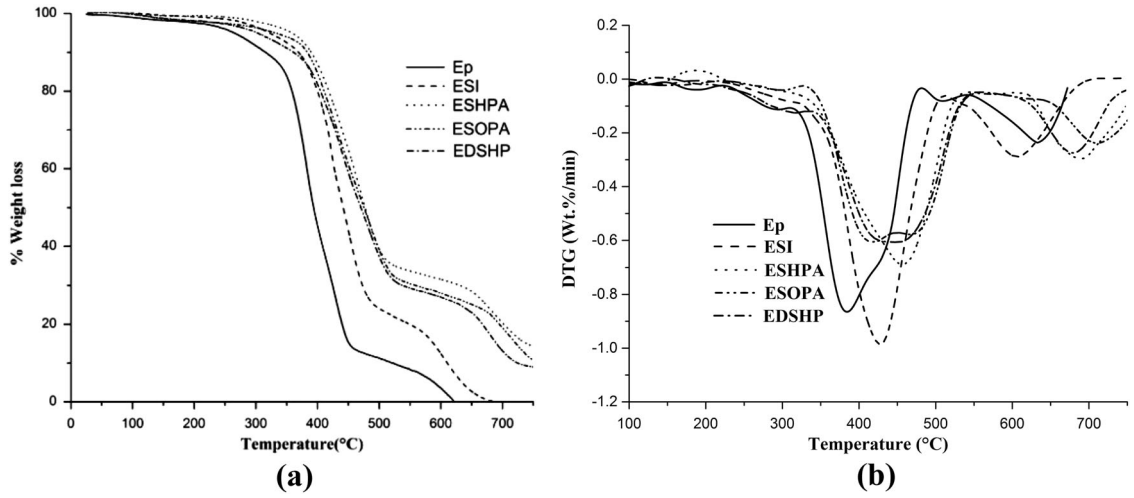

Fig. 7 **a** TGA curves of composites **b** DTG curves of composites

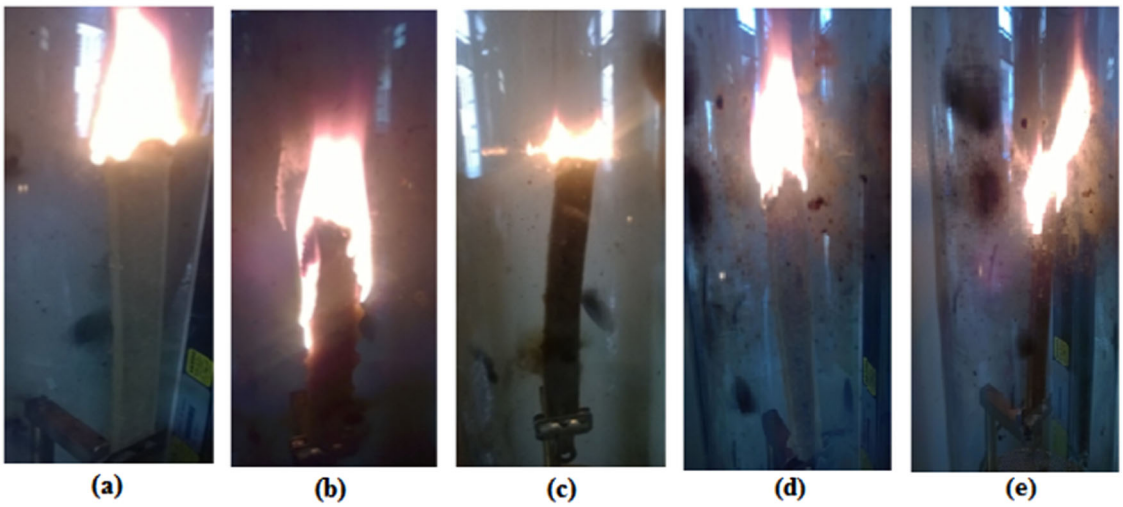

Fig. 8 Burning behavior of pure epoxy and composites **a** Ep **b** ESI **c** ESHPA **d** ESOPA **e** EDSHP

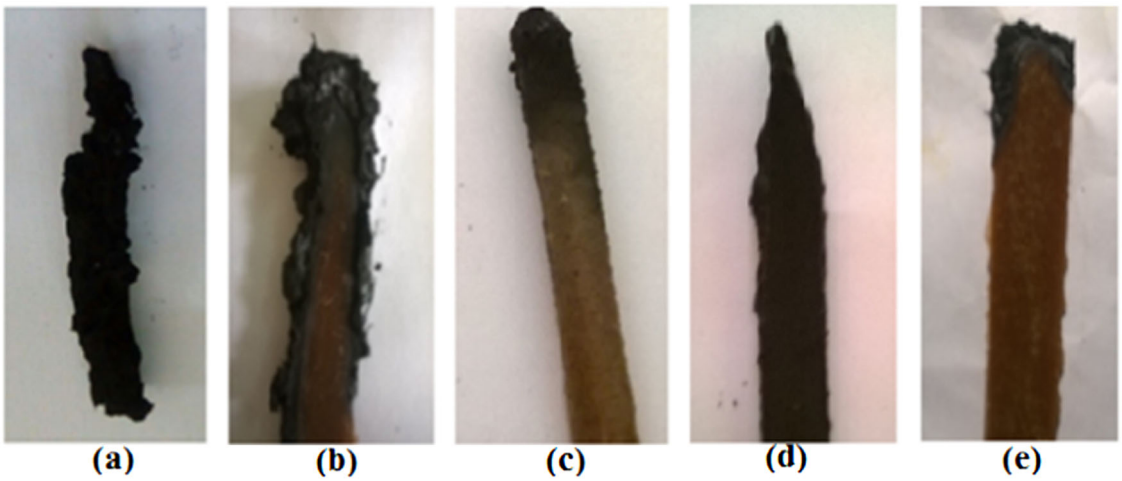

Fig. 9 Photos of burnt sample after LOI test for pure Epoxy and composites **a** Ep **b** ESI **c** ESHPA **d** ESOPA **e** EDSHP

laboratory conditions. The measurements are made regarding the loss of light transmission through a collected volume of smoke produced under-regulated and standardized conditions. The samples have dimensions $25 \times 25 \times 6$ mm.

The average values of the percentage absorption and the nature of the graph indicate the value of maximum smoke density to be 100 (Fig. 12). The color of the flame was orange, and the smoke color was black. Thus it can be said that the smoke was very dense. This is due to the incomplete combustion of the aromatic system of the resin [40, 41].

4 Conclusions

Phosphorous containing silica powder was prepared successfully by acid hydrolysis of sodium silicate in the presence of Di-sodium hydrogen orthophosphate, orthophosphoric acid, and hypophosphorous acid. FTIR spectra show the presence of phosphate group in the silica matrix. TGA curve shows higher residue for phosphorous containing silica than pure silica at 700 °C. SEM picture of phosphorous containing silica has globular structure compare to the fluffy structure of pure silica. EDX result shows 2–5% atomic weight of phosphorous in phosphorous-containing silica. The XRD results indicate the amorphous nature of the powdered silica whereas phosphorous-containing silica shows three sharp spikes at 2Θ, 31, 45, and 56 degrees respectively. This is due to the formation of three-dimensional structure generated by the reaction of hydroxyl groups between phosphorous and silicon. The particle size of all the samples was nearly 1000 nm but the porosity determined by mercury porosity meter of the phosphorous containing particles was lower than pure silica.

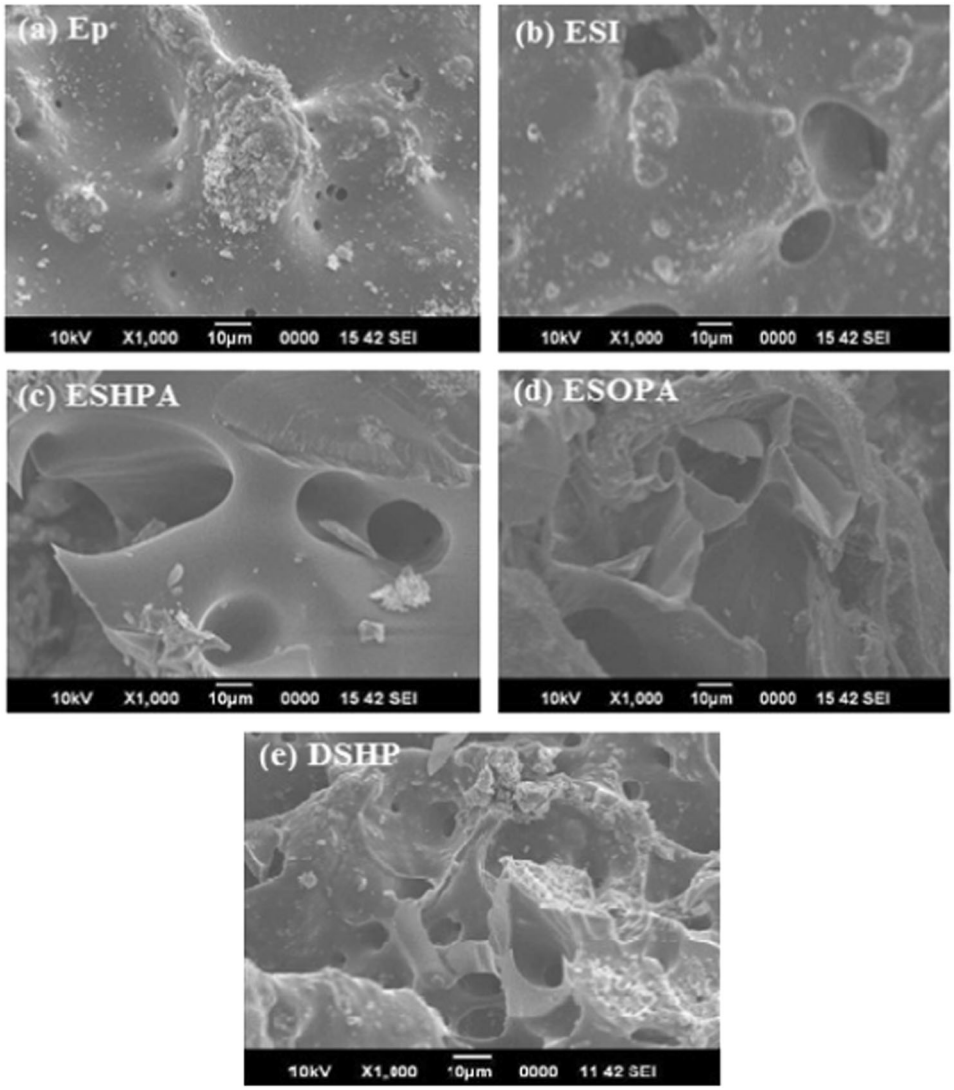

Fig. 10 SEM of char formed of burnt sample after LOI test for pure Epoxy and composites

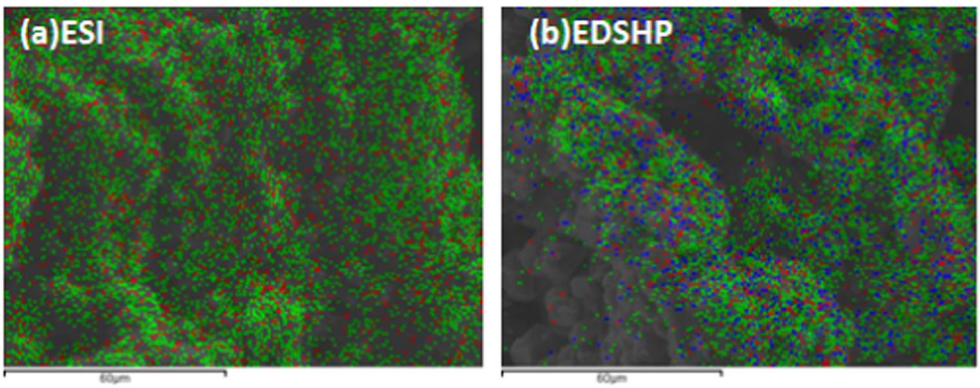

Fig. 11 Si and P-mapping of char of composites (silicon green color, oxygen red color, and phosphorous blue color) (color figure online)

Epoxy composite with pure silica and phosphorous containing silica were prepared and characterized by TGA, LOI, and smoke density. TGA patterns of the composites are almost same up to 450 °C. At this temperature residue for phosphorous containing sample is 20% higher than epoxy-silica composites. Above this temperature phosphorous containing sample shows a slow rate of degradation up to 600 °C. Finally, the residue at 650 °C for phosphorous

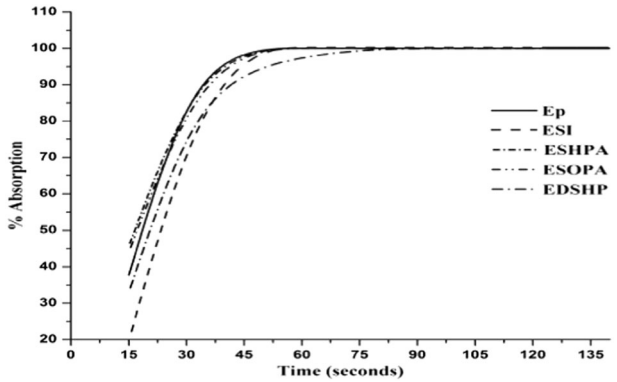

Fig. 12 Light absorption verses time of the specimen in smoke density tester

containing sample is 10–14% higher than epoxy-silica composites. The flame behavior in LOI test shows less flame propagation due to the formation of char. The SEM pictures of char explain the formation of bubbles in the phosphorous containing samples. The foamed structure of char is responsible for the slow propagation of flame.

Acknowledgements The authors are gratefully acknowledge the financial support from NRB DRDO sponsored project (NRB/4003/PG/340). The authors are also acknowledge the characterization facility (Central Instrumentation Facility) at Birla Institute of Technology Mesra.

Compliance with ethical standards

Conflict of interest The authors declare that they have no competing interests.

References

1. Chen X, Gu A, Liang G, Yuan L, Zhuo D, Hu JT (2012) Novel low phosphorus-content bismaleimide resin system with outstanding flame retardancy and low dielectric loss. Polym Degrad Stab 97(5):698–706
2. Klinkowski C, Wagner S, Ciesielski M, Doring M (2014) Bridged phosphorylated diamines: synthesis, thermal stability and flame retarding properties in epoxy resins. Polym Degrad Stab 106:122–128
3. Wang T, Wan PY, Qin PY, Yu M (2008) Synthesis and characterization of dicyclopentadiene–cresol epoxy resin. Poly Bull 59 (6):787–793
4. Gao LP, Wang DY, Wang YZ, Wang JS, Yang B (2008) A flame-retardant epoxy resin based on a reactive phosphorus-containing monomer of DODPP and its thermal and flame-retardant properties. Polym Degrad Stab 93(7):1308–1315
5. El Gouri M, El Bachiri A, Hegazi SE, Rafik M, El Harfi A (2009) Thermal degradation of a reactive flame retardant based on cyclotriphosphazene and its blend with DGEBA epoxy resin. Polym Degrad Stab 94(11):2101–2106
6. Gu L, Chen G, Yao Y (2014) Two novel phosphorus–nitrogen-containing halogen-free flame retardants of high performance for epoxy resin. Polym Degrad Stab 108:68–75
7. Sen AK, Kumar S (2010) Coir-fiber-based fire retardant nano filler for epoxy composites. J Therm Anal Calorim 101 (1):265–271
8. Liang S, Neisius NM, Gaan S (2013) Recent developments in flame retardant polymeric coatings. Prog Org Coat 76 (11):1642–1665
9. Balabanovich AI, Hornung A, Merz D, Seifert H (2004) The effect of a curing agent on the thermal degradation of fire retardant brominated epoxy resins. Polym Degrad Stab 85 (1):713–723
10. Covaci A, Voorspoels S, Abdallah MA, Geens T, Harrad S, Law RJ (2009) Analytical and environmental aspects of the flame retardant tetrabromobisphenol-A and its derivatives. J Chromatogr A 1216(3):346–363
11. Buczko A, Stelzig T, Bommer L, Rentsch D, Heneczkowski M, Gaan S (2014) Bridged DOPO derivatives as flame retardants for PA6. Polym Degrad Stab 107:158–165
12. Lu SY, Hamerton I (2002) Recent developments in the chemistry of halogen-free flame retardant polymers. Prog Polym Sci 27 (8):1661–1712
13. Schartel B (2010) Phosphorus-based flame retardancy mechanisms—old hat or a starting point for future development? Mater J 3(10):4710–4745
14. Jeng RJ, Shau SM, Lin JJ, Su WC, Chiu YS (2002) Flame retardant epoxy polymers based on all phosphorus-containing components. Eur Polym J 38(4):683–693
15. Dong Q, Liu M, Ding Y, Wang F, Gao C, Liu P, Wen B, Zhang S, Yang M (2013) Synergistic effect of DOPO immobilized silica nanoparticles in the intumescent flame retarded polypropylene composites. Polym Adv Technol 24(8):732–739
16. Chen Y, Zhan J, Zhang P, Nie S, Lu H, Song L, Hu Y (2010) Preparation of intumescent flame retardant poly (butylene succinate) using fumed silica as synergistic agent. Ind Eng Chem Res 49(17):8200–8208
17. Alongi J, Colleoni C, Rosace G, Malucelli G (2012) Thermal and fire stability of cotton fabrics coated with hybrid phosphorus-doped silica films. J Therm Anal Calorim 110(3): 1207–1216
18. Shewale PM, Rao AV, Rao AP, Bhagat SD (2009) Synthesis of transparent silica aerogels with low density and better hydrophobicity by controlled sol–gel route and subsequent atmospheric pressure drying. J Sol–Gel Sci Technol 49(3):285–292
19. Lin YS, Lin HP, Mou CY (2004) A simple synthesis of well-ordered super-microporous aluminosilicate. Microporous Mesoporous Mater 76(1):203–208
20. Meenakshi KS, Sudhan EP, Kumar SA (2012) Development and characterization of new phosphorus based flame retardant tetraglycidyl epoxy nanocomposites for aerospace application. Bull Mater Sci 35(2):129–136
21. Giraldo L, Bastidas-Barranco M, Moreno-Pirajan JC (2016) Adsorption calorimetry: energetic characterisation of the surface of mesoporous silicas and their adsorption capacity of non-linear chain alcohols. Colloids Surf A 496:100–113
22. Dong Q, Ding Y, Wen B, Wang F, Dong H, Zhang S, Wang T, Yang M (2014) Improvement of thermal stability of polypropylene using DOPO-immobilized silica nanoparticles. Colloid Polym Sci 290(14):1371–1380
23. Music S, Filipovic-Vincekovic N, Sekovanic L (2011) Precipitation of amorphous SiO_2 particles and their properties. Braz J Chem Eng 28(1):89–94
24. Bryans TR, Brawner VL, Quitevis EL (2000) Microstructure and porosity of silica xerogel monoliths prepared by the fast sol–gel method. J Sol–Gel Sci Technol 17(3):211–217
25. Kalapathy U, Proctor A, Shultz J (2000) A simple method for production of pure silica from rice hull ash. Biores Technol 73 (3):257–262

26. Olhero SM, Ferreira JM (2004) Influence of particle size distribution on rheology and particle packing of silica-based suspensions. Powder Technol 139(1):69–75
27. Jesionowski T, Krysztafkiewicz A (2002) Preparation of the hydrophilic/hydrophobic silica particles. Colloids Surf A 207 (1):49–58
28. Massiot P, Centeno MA, Gouriou M, Dominguez MI, Odriozola JA (2003) Sol–gel obtained silicophosphates as materials to retain caesium at high temperatures. J Mater Chem A 13 (1):67–74
29. Massiot P, Centeno MA, Carrizosa I, Odriozola JA (2001) Thermal evolution of sol–gel-obtained phosphosilicate solids (SiPO). Non-Cryst Solids 292(1):158–166
30. Wang X, Hu Y, Song L, Xing W, Lu H, Lv P, Jie G (2010) Flame retardancy and thermal degradation mechanism of epoxy resin composites based on a DOPO substituted organophosphorus oligomer. Polym 51(11):2435–2445
31. Liu YL, Wei WL, Hsu KY, Ho WH (2004) Thermal stability of epoxy-silica hybrid materials by thermogravimetric analysis. Thermochim Acta 412(1):139–147
32. Liu YL, Hsu CY, Wei WL, Jeng RJ (2003) Preparation and thermal properties of epoxy-silica nanocomposites from nanoscale colloidal silica. Polymer 44(18):5159–5167
33. Ho TH, Hwang HJ, Shieh JY, Chung MC (2009) Thermal, physical and flame-retardant properties of phosphorus-containing epoxy cured with cyanate ester. React Funct Polym 69(3):176–182
34. Cavdar AD (2014) Effect of various wood preservatives on limiting oxygen index levels of fire wood. Measurement 50:279–284
35. Suzanne M, Delichatsios MA, Zhang JP (2014) Flame extinction properties of solids obtained from limiting oxygen index tests. Combust Flame 161(1):288–294
36. Qian X, Song L, Hu Y, Jiang S (2016) Novel DOPO-based epoxy curing agents. J Therm Anal Calorim 126(3):1339–1348
37. Qian X, Song L, Hu Y, Yuen RK (2013) Thermal degradation and flammability of novel organic/inorganic epoxy hybrids containing organophosphorus-modified oligosiloxane. Thermochim Acta 552:87–97
38. Alongi J, Collconi C, Rosace G, Malucelli G (2012) Thermal and fire stability of cotton fabrics coated with hybrid phosphorus-doped silica films. J Therm Anal Calorim 110:1207–1216
39. Chiang C, Ma C (2002) Synthesis, characterization and thermal properties of novel epoxy containing silicon and phosphorous nanocomposites by sol–gel method. Eur Polym J 38:2219–2224
40. Wang X, Hu Y, Song L, Yang H, Xing W, Lu H (2011) Synthesis and characterization of a DOPO-substitued organophosphorus oligomer and its application in flame retardant epoxy resins. Prog Org Coat 71(1):72–82
41. Sponton M, Ronda JC, Galia M, CAdiz V (2009) Cone calorimetry studies of benzoxazine–epoxy systems flame retarded by chemically bonded phosphorus or silicon. Polym Degrad Stab 94 (1):102–106